

Oscar González-Martín
 Carlos Oteo
 Ricardo Ortega
 Javier Alandez
 Mariano Sanz
 Mario Veltri

Evaluation of peri-implant buccal bone by computed tomography: an experimental study

Authors' affiliations:

Oscar González-Martín, Department of Periodontics, University of Pennsylvania Dental School, Philadelphia, PA, USA
 Oscar González-Martín, Mariano Sanz, Department of Periodontology, University Complutense of Madrid, Madrid, Spain
 Carlos Oteo, Department of Esthetic Dentistry, University Complutense of Madrid, Madrid, Spain
 Ricardo Ortega, Department of Radiology, University Complutense of Madrid, Madrid, Spain
 Javier Alandez, Private Practice, Madrid, Spain
 Mario Veltri, Specialist Clinic for Periodontology, Goteborg, Sweden

Corresponding author:

Oscar González-Martín, DDS, MSc
 Postdoctoral Periodontal-Prosthesis Program
 Department of Periodontics
 University of Pennsylvania School of Dental Medicine
 240 South 40th Street
 Philadelphia, PA 19104-6030
 USA
 Tel.: +1 2158987991
 Fax: +1 2155733939
 e-mail: oscargm76@yahoo.es

Key words: cone-beam CT, cortical bone, dental implant

Abstract

Objectives: To evaluate the accuracy of measuring peri-implant buccal bone when using three different computed tomography devices.

Materials and methods: Sixty tissue-level or bone-level dental implants were placed in bovine ribs with either buccal bone full coverage, dehiscence or fenestration. For each site, the distance from the bone defect to the implant neck and the buccal bone thickness 1 mm apical to the crest were measured using a calliper. Subsequently, all sites were scanned in a reproducible position using a multi-slice computed tomography (CT) (Brightspeed, voxel size 0.625 mm) and two cone-beam computed tomography devices (i-CAT NG, voxel size 0.3 mm and Newtom VGi, voxel size 0.2 mm). Bone thickness was measured on images from the three systems similar to direct measurements and differences were evaluated. Factors that could influence the buccal bone identification were assessed by multiple binary logistic regression.

Results: Buccal bone ranged from 0.1 mm to 2.75 mm in thickness and was not visible in 68%, 63% and 60% of cases when using CT, i-CAT and Newtom, respectively. For each mm of bone thickness increment, the odds of radiographic identification increased by 30.6 ($P < 0.001$). Bone defects negatively affected radiographic visibility ($P < 0.05$). All devices underestimated bone dimensions although differences among them were not significant.

Conclusions: Within these experimental conditions, the investigated devices have equivalent low accuracy in diagnosing peri-implant buccal bone. Accuracy was significantly influenced by buccal bone thickness, especially if <1 mm, and in presence of peri-implant marginal defects.

Peri-implant buccal bone thickness is usually assessed during implant installation or the second stage surgery in submerged implant protocols, but it is seldom evaluated thereafter since conventional oral radiographic diagnosis only evaluates interdental marginal bone levels. This factor, however, may have important implications for the long-term stability of both peri-implant hard and soft tissues. In sites where the buccal bone thickness was <1.5 mm during the second stage surgery, there was frequently bone loss and dehiscence (exposed implant surface), while as the buccal bone thickened (between 1.8 to 2 mm), the occurrence of dehiscence decreased significantly (Spray et al. 2000).

The long-term influence of the buccal bone thickness has been assessed by Schwarz et al. (2012) who evaluated the impact of residual marginal bone dehiscence after guided bone regeneration on the long-term stability of

peri-implant health, reporting that implants exhibiting residual defects of more than 1 mm in height were at higher risks of presenting mucosal clinical attachment loss, marginal recession and deepened probing pocket depths, 4 years after treatment. These complications are of greater importance in the anterior maxilla where the bucco-lingual bone dimensions are limited (Huynh-Ba et al. 2010) and where the aesthetic outcomes are a priority, but there is no evidence on the minimal bone thickness needed to ensure optimal aesthetics (Teughels et al. 2009; Merheb et al. 2014).

The introduction of computed tomography (CT) for diagnosis in implant therapy (Schwarz et al. 1987a,b) has allowed a three-dimensional visualisation of the bone, particularly in the bucco-lingual direction, which previously was not possible with traditional radiological techniques. Cone-beam

Date:

Accepted 13 June 2015

To cite this article:

González-Martín O, Oteo C, Ortega R, Alandez J, Sanz M, Veltri M. Evaluation of peri-implant buccal bone by computed tomography: an experimental study. *Clin. Oral Impl. Res.* 27, 2016, 950–955
 doi: 10.1111/clr.12663

computed tomography (CBCT) has significantly widened the use of CT images in implant dentistry due to potentially reduced radiation dosage and cost. Nonetheless, CBCT images of peri-implant bone might be affected by artefacts that may result in incorrect bone grey values and consequently, erroneous reconstructions (Schulze et al. 2011; Benic et al. 2013) and imprecise diagnosis (Zhang et al. 2007). The accuracy of computed tomography for evaluation of peri-implant bone has been tested in different experimental models. When implants were placed in animal ribs, peri-implant buccal bone could be visualised on CBCT images with good accuracy only when the bone was of sufficient thickness (Razavi et al. 2010). Similar conclusions were reached when implants were placed in dry skulls (Shiratori et al. 2012). Even though the buccal bone thickness around dental implants has been extensively evaluated with CBCT (Nisapakultorn et al. 2010; Kehl et al. 2011; Miyamoto & Obama 2011; Benic et al. 2012; Degidi et al. 2012; Vera et al. 2012; Buser et al. 2013a,b; Lee et al. 2014; Jung et al. 2015), there are still questions on its reproducibility and the possible effects of artefacts in sites with thin buccal bone plates (Spin-Neto et al. 2011).

It is therefore the objective of this experimental study to investigate the effect of bone thickness on the accuracy of peri-implant buccal bone evaluation by means of computed tomography. Furthermore, the influence of the bucco-lingual implant position, the implant emergence profile and the radiographic device used will be evaluated.

Material and methods

Experimental design

Dental implants were placed in fresh bovine ribs using a previously reported protocol (Razavi et al. 2010). In brief, 10 fresh bovine ribs obtained from a local slaughterhouse were denuded from soft tissues and their base was flattened to obtain a stable horizontal position for implant placement and CBCT scanning. A marker was used to distinguish between the left and right side of the rib, and once the implants were inserted, the anterior aspect of the rib represented the buccal bone plate, while the posterior aspect represented the lingual bone plate. For reproducible implant positioning, a guide was created for each single rib using silicon impression putty (Flexitime, Heraeus, South Bend, IN, USA). Ribs were kept frozen between the different

phases of the experiment. A total of 30 bone-level implants (SLA, Institut Straumann AG, Basel, Switzerland) and 30 tissue-level implants (Standard implants, SLA, Institut Straumann AG) were placed in the prepared ribs. The drilling sequence started at the superior border of the bovine ribs following the manufacturer's instructions (Institut Straumann AG). Tissue-level implants were placed with the polished collar supracrestally, while bone-level implants were placed at bone level. The distance between implants was 10 mm or more. Implants were inserted in three different positions in the bucco-lingual dimension to create three different peri-implant outcomes in the buccal surface: (a) 20 implants with full buccal bone coverage, (b) 20 implants with dehiscence defects, and (c) 20 implants with fenestration defects. In each group, 10 implants were tissue level and 10 bone level. In the group of complete bone coverage, implants were placed at various distances from the outer bone surface to create different buccal bone thicknesses.

Once the implant sites were prepared and before implant placement, direct measurements of the buccal bone thickness 1 mm apical to the crest were performed using a digital calliper (Mestra®, Bilbao, Spain) (Fig. 1a). This direct measurement was the gold standard for subsequent radiographic comparisons. After implant installation, the distance from the implant neck to the buccal bone defect was measured (Figs 1b,c and 3 left column). The ribs were then transported to the radiological centre under refrigeration to minimise the loss of moisture and were covered with a layer of wax (1.5 mm of thickness) (Tenatex Red, Kemdent Works, Swindon, UK) to simulate the soft tissue covering the alveolar bone and thus attaining a similar beam attenuation (Shmueli et al. 2007).

A customised plastic box housing the silicon guides holding the ribs was used during the scanning for assuring reproducible positioning of the ribs in the three radiology devices. Three computed tomography devices were used: one multi-slice CT Scanner (Brightspeed 16, General Electric Medical Systems, Milwaukee, WI, USA) and two CBCT devices: i-CAT NG (Imaging Sciences International, Hatfield, PA, USA) and NewTom VGi (QR, Verona, Italy).

The detailed settings for these devices were as follows:

- CT scan 120 kV and 60 mA, voxel size 0.625 mm, acquisition time 4 s, FOV 13.9 cm × 13.9 cm and slice thickness 0.3 mm.
- i-CAT NG 110 kV and 2–3.20 mA, voxel size 0.3 mm, acquisition time 4.8 s, FOV 16 cm × 6 cm and slice thickness 0.3 mm.
- Newtom VGi 110 kV and 4 mA, voxel size 0.2 mm, acquisition time 5.4 s, FOV 15 cm × 15 cm and slice thickness 0.3 mm.

A trained specialist in oral radiology (RO) carried out all the scans and securely stored all obtained images in a computer hard disk (SanDisk, Milpitas, CA, USA) containing a software for image analysis (NNT Software 5.0, QR, Verona, Italy) (Fig. 2).

For each implant, a cross-sectional image, as closely as possible through the implant centre, was selected and two examiners experienced in 3D imaging and CBCT diagnosis (one specialist in oral radiology [RO] and one specialist in periodontology [OG]) carried out in parallel all the measurements. In case of discrepancy, the decision was made by consensus. When bone was visible at the buccal bone surface, the examiners evaluated its thickness from the outer implant surface

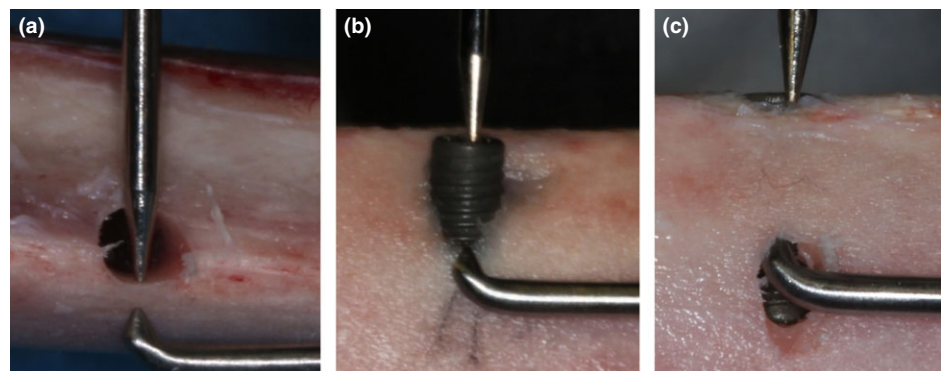


Fig. 1. Clinical images of the direct measurements using the digital calliper to record the thickness 1 mm apical to the crest in a case of complete bone coverage of the implant (a) and the distance from the implant neck to the defect in a case of dehiscence (b) and fenestration (c).

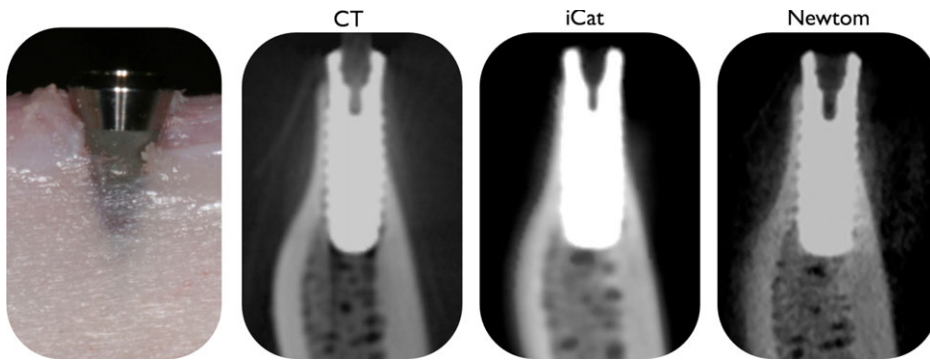


Fig. 2. Clinical view of an implant presenting a dehiscence (2.93 mm from the neck of the implant to the bone) and a thin buccal plate measured 1 mm apical to the defect (0.11 mm) and corresponding radiological analysis (from left to right: CT scan, i-CAT NG and Newtom VGi). Observe that radiographically visible buccal plate starts at 7.8 mm, 7.9 mm and 8.4 mm, respectively, from the neck of the implant.

1 mm apical to the bone crest (Fig. 3). The contrast and brightness of the images were preset in the software to provide constant viewing settings during the examinations.

Data analysis

A multiple binary logistic regression model was applied to assess the factors influencing the probability of identifying the buccal bone on 3D X-rays at the level of 1 mm below the

marginal crest. Buccal bone identification (yes/no) was the binary outcome variable. The following explanatory factors were evaluated to assess the probability for positive buccal bone identification: buccal bone thickness, buccal bone level (vertical distance of the defect from the implant neck), peri-implant buccal bone position (full coverage, fenestration, dehiscence), implant design (tissue level, bone level) and computed

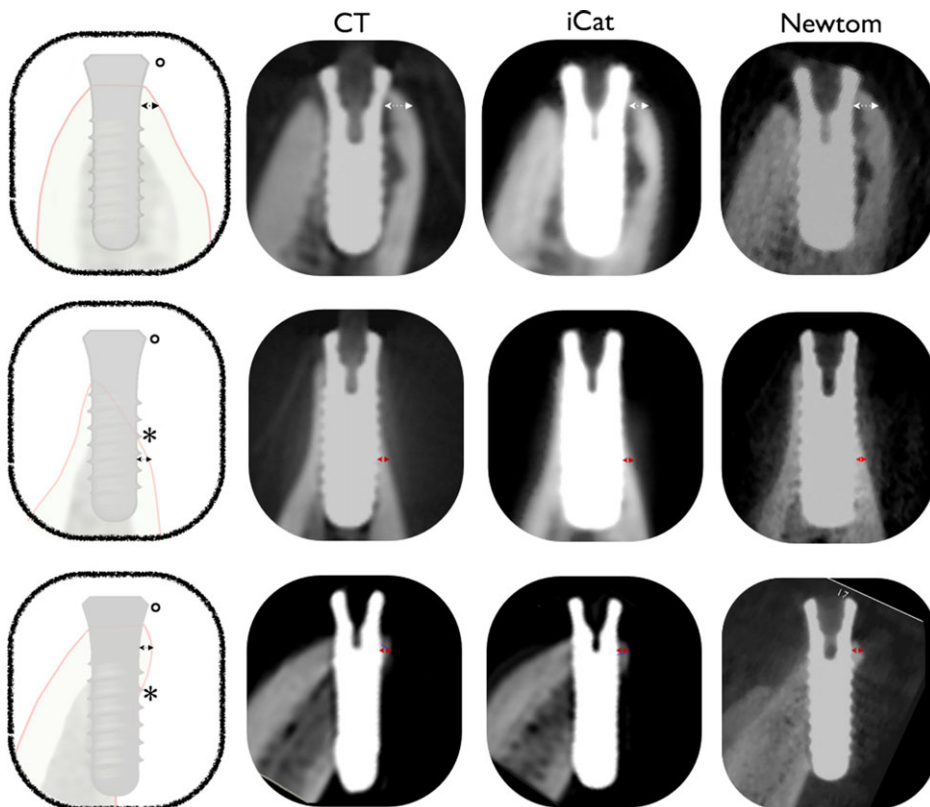


Fig. 3. Designs on the left show direct measurements by calliper on implants fully in bone or with dehiscence. The distance of the defect from the implant neck was measured from the implant neck (circle) to the bone defect (asterisk). Buccal bone crest thickness was measured 1 mm apically to the buccal bone level (arrow). On the right, radiographic images from the different systems tested. Buccal bone thickness (arrow) was measured 1 mm apically to the bone level reproducing direct measurement.

tomography device (CT, i-CAT, Newtom). Covariates were entered into the model using a backward stepwise method by means of the Wald test.

Wilcoxon signed rank tests were utilised to assess differences in buccal bone thickness evaluated by direct measurements (gold standard) and by the three radiographic systems. Paired analysis using the same statistical test was performed after stratifying the samples according to thickness (<1 mm vs. ≥1 mm thick). The thicker samples (≥1 mm) were further stratified as fully covered vs. marginal defects (dehiscence and fenestration).

All statistical analyses were performed using the software SPSS Statistics 21 (IBM Company Inc. Chicago, IL, USA).

Results

A total of 60 rib bone-implant specimens were evaluated. Table 1 depicts the direct peri-implant buccal bone dimensions measured before implant placement. Buccal bone thicknesses 1 mm apical to the bone crest ranged between 0.1 and 2.75 mm. Table 2 depicts the mean buccal bone thicknesses measured with the 3 tomographic devices once the implants were placed. When compared to the direct measurements, images obtained by CT, i-CAT and Newtom significantly underestimated the buccal bone, as it was not radiographically visible in 67% of the cases. Depending on the CT device used, it was not visible by CT in 41 cases (68%), by i-CAT in 38 cases (63%) and by Newtom in 36 cases (60%). There were no significant differences among the three devices. In the paired analysis, the evaluation of the thin subgroup (<1 mm) rendered a substantial underestimation for all three radiographic systems when compared with the direct measurements, but differences were not significant between systems themselves. Similarly, the analysis of the thicker subgroup (≥1 mm) showed a significant underestimation when compared to the gold standard. A significant underestimation resulted also when the analysis was repeated for subgroups with or without marginal bone defects.

The result of the multiple binary logistic regression model was that the implant design (tissue level versus bone level) as well as the position of the implant (vertical distance from the implant neck to the buccal bone crest) did not influence significantly the probability of buccal bone identification. The bone thickness, however, had a significant influence on the radiographic visibility. Figure 4

Table 1. Descriptive statistics for peri-implant bone anatomy as assessed by direct measurements in the different experimental groups

	Buccal thickness				Bone-level implants	Tissue-level implants	Vertical distance from defect
	Overall	No defects	Dehiscence	Fenestration			
Mean	0.83	0.97	0.88	0.65	0.96	0.57	6.64
SD	0.78	0.62	0.92	0.78	0.94	0.72	2.24

graphically depicts the probability of being radiographically visible depending on the buccal bone thickness. For sites with 0.5 mm, the probability was less than 20%, while when the thickness was 2.75 mm, it was identified in 100% of the cases. For each mm increase in bone thickness, the odds of bone identification increased by 30.6 ($P < 0.001$). The presence of marginal buccal bone defects also had a significant negative impact on the probability of radiographic visibility ($P < 0.05$). Figure 5 illustrates the predicted probability of radiographic identifiability for various bone thicknesses at sites with or without marginal defects. A test of the final model versus a model with intercept only was statistically significant χ^2 ($N = 180$) = 127.56; $P < 0.01$. The model was able to correctly classify 91% of the cases when bone was radiographically identifiable and 92% of the cases when bone was radiographically not visible for an overall success rate of 91.7%. Table 3 shows the logistic regression coefficient and odds ratio for each of the covariates in the final model.

Discussion

The possible influence of the peri-implant buccal bone dimensions on the stability of the peri-implant hard and soft tissues has

been studied using conventional or cone-beam CT in several clinical investigations (Nisapakultorn et al. 2010; Benic et al. 2012; Miyamoto & Obama 2011; Kehl et al. 2011; Degidi et al. 2012; Vera et al. 2012; Buser et al. 2013a, 2013b; Lee et al. 2014; Jung et al. 2015). These studies, however, did not consider the influence of the accuracy and reproducibility of the radiological devices used and other possible factors that may have influenced the validity of these CT measurements.

In this *in vitro* experimental study, we have demonstrated a significant underestimation of the buccal bone identification around dental implants irrespective of the CT device tested. Moreover, we have shown that the visibility of the peri-implant buccal bone depends on the thickness of the buccal bone and on the integrity of coronal buccal bone around the implant neck. The animal experimental model was chosen based on a previous similar investigation (Razavi et al. 2010) and on the fact that rib bones have a similar bone architecture to human jaws (May et al. 1997; Choi et al. 2005; Chiodo et al. 2006). Under these experimental conditions, the conventional and the two cone-beam CTs, resulted in an underestimation of the dimension of the buccal bone, when compared with direct measurements, in fact, the peri-implant buccal bone dimension was significantly smaller or

not visible when assessed radiographically. As shown by regression analysis in Figs 4 and 5, above 1 mm of thickness the probability of buccal bone being radiographically visible increased beyond 50%. This finding conforms to previous observations by Razavi et al. (2010) that above 1 mm of thickness, the accuracy of CBCT images increased substantially. As a consequence, the 1 mm value was chosen as a threshold for stratifying in a thicker and thinner subgroup and thus evaluates the accuracy of the radiographic measurements. On the other hand, the error reported in this investigation (85.7%) for the i-CAT in the thin subgroup (<1 mm) was slightly higher than the one reported by Razavi et al. (2010) (68%) for bone thicknesses ranging between 0.04 and 1.99 mm. These differences could be due to differences in the peri-implant bone anatomy. This low accuracy of CT images in thin ridges is particularly relevant for implants located in the anterior maxilla, as different studies in humans have reported that buccal bone crests having thicknesses of 1 mm or less occur in more than 85% of the implant sites (Huynh-Ba et al. 2010; Januário et al. 2011).

Beside buccal bone thickness, factors such as implant emergence profile, presence of peri-implant bone defects (such as dehiscence and fenestrations) and the vertical distance between the implant neck to the crest may also affect the visibility of the buccal bone as assessed by the three different radiological systems. From the multiple regression analysis performed, it resulted that the factors significantly affecting buccal bone visibility were the buccal bone thickness and the presence of marginal bone defects. When marginal defects were present, the probability of being radiographically visible was clearly reduced

Table 2. Direct (gold standard) and radiographic mean buccal bone thickness (mm) for the whole sample and for subgroups with different marginal bone configurations

N	All implants		Implants with <1 mm bone thickness		Implants with ≥ 1 mm bone thickness		Implants with ≥ 1 mm thickness & no defects		Implants with ≥ 1 mm thickness & marginal defects	
	60		43		17		7		10	
	Mean	SD	Mean	SD	Mean	SD	Mean	SD	Mean	SD
Gold standard	0.83*	0.78	0.39*	0.25	1.94*	0.5	1.67*	0.4	2.14*	0.48
CT	0.43*	0.76	0.03*	0.14	1.43*	0.8	1.46*	0.4	1.41*	0.96
Δ CT	0.41	0.40	0.4	0.25	0.51	0.6	0.2	0.1	0.7	0.77
% error CT	76.20%		92.87%		26.39%		12.52%		33.96%	
i-CAT	0.44*	0.74	0.06*	0.16	1.41*	0.7	1.50*	0.4	1.37*	0.89
Δ i-CAT	0.39	0.40	0.3	0.29	0.55	0.5	0.2	0.1	0.8	0.68
% error i-CAT	72.90%		85.75%		28.53%		9.95%		35.83%	
Newtom	0.44*	0.69	0.08*	0.21	1.35*	0.7	1.54*	0.4	1.21*	0.79
Δ Newtom	0.39	0.39	0.3	0.21	0.59	0.6	0.1	0.1	0.9	0.61
% error Newtom	69.80%		78.62%		39.63%		7.38%		43.33%	

* $P < 0.05$ Wilcoxon signed rank test.

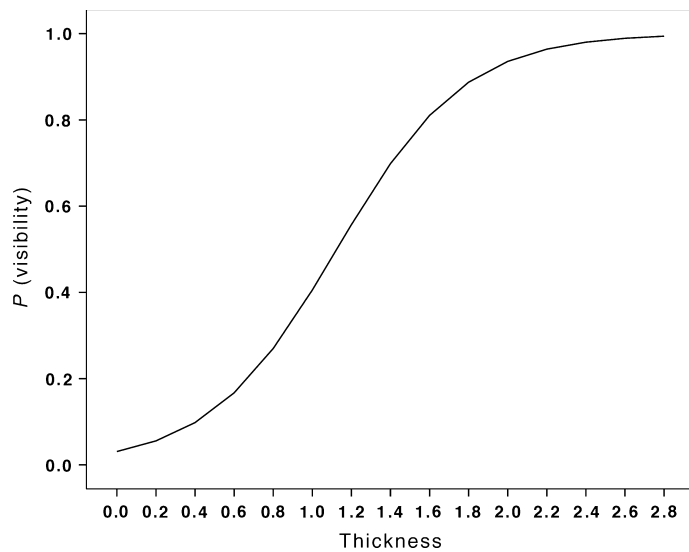


Fig. 4. Probability of buccal bone identification according to the buccal bone thickness (mm) as measured directly by calliper.

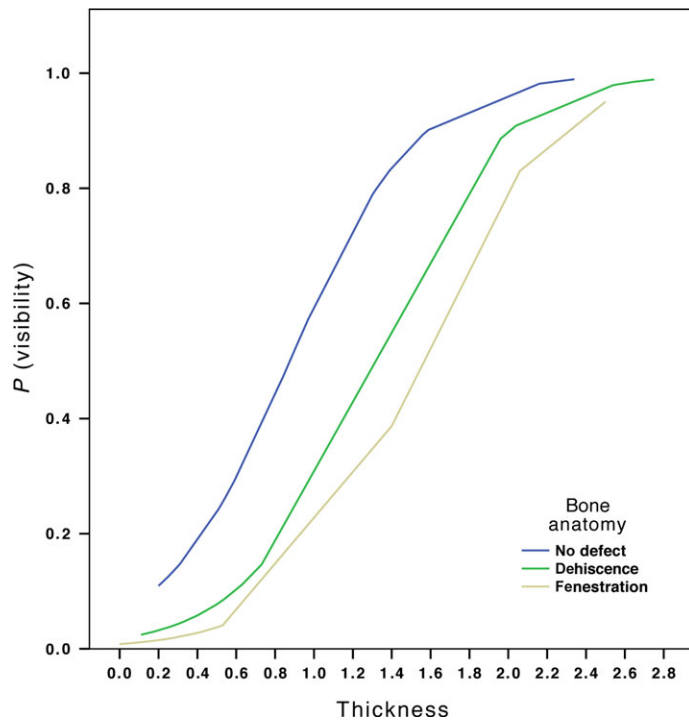


Fig. 5. Probability of buccal bone identification according to the buccal bone thickness (mm) as measured directly by calliper for sites with or without marginal bone defects.

Table 3. Backward stepwise multiple logistic regression model with “non-identifiable”/“identifiable” buccal bone as the dependent variable. Among the independent variables, “tissue-level implant design” and “no buccal bone defects” were reference categories

Variable	Coefficient	SE	P value	Odds ratio	95% CI
Thickness (mm)	3.422	0.547	0.000	30.639	10.487/89.515
Implant design					
Tissue level				1	
Bone level	1.051	0.552	0.057	2.859	0.969/8.439
Buccal bone					
No defect				1	
Dehiscence	-3.709	1.485	0.013	0.025	0.001/0.450
Fenestration	-4.982	1.747	0.004	0.007	0.000/0.211
Distance from defect (mm)	0.451	0.248	0.69	1.570	0.965/2.554

when compared with marginally intact sites. A separate analysis of specimens with a thickness ≥ 1 mm without or with marginal bone defects (dehiscence or fenestration) showed that measurements were always significantly different from the gold standard for any of the three CT units; however, errors were in a lower range when specimens without defects were assessed. In particular, the Newtom showed a tendency for less percentage error in sites with a buccal bone wall thicker than 1 mm and without marginal defects. This device was studied in a previous study reporting that the occurrence of beam hardening artefacts affecting peri-implant bone images was less significant in this device when compared to devices using lower kV (Esmaeili et al. 2012). However, no previous studies have assessed the accuracy of peri-implant buccal bone measurements using the newer Newtom VGi device. The same applies for the Brightspeed CT device. With regard to the i-CAT, a previous study evaluated its accuracy for measuring the buccal bone volume around dental implants placed in dried skulls (Shiratori et al. 2012). A good accuracy and reproducibility of the i-CAT was reported; however, buccal bone thickness ranged from 1.2 to 4.76 mm as compared to thicknesses between 0.1 and 2.76 mm in the present investigation.

Despite the study was not designed to assess the possible effect of artefacts and the influence of different fields of view (FOV) and voxel sizes in the three systems used, they may have indeed influenced the outcome. It has been proposed that the image quality from CBCT devices is less prone to metallic artefacts compared to multi-slice CT (Holberg et al. 2005). On the contrary, other studies outlined how in presence of metal, more artefacts may influence the accuracy of CBCT images, such as aliasing artefacts due to the cone-beam divergence, scatter and an overall higher noise level (Schulze et al. 2010; Schulze et al. 2011). In the present study, despite artefacts were not qualitatively assessed, multi-slice CT accuracy did not appear to differ from that of CBCT devices, when assessing peri-implant buccal bone. Similar considerations may apply for FOV and voxel sizes. Three different FOV and voxel sizes were used in the three different CT devices tested, nonetheless significant differences in accuracy did not occur. A recent literature review discussed how smaller FOV and voxel sizes could produce sharper images but still allowing the same diagnostic outcome as larger voxel images (Spin-Neto et al. 2013). When considering how FOV and voxel

sizes affect the radiation dose to the patient, it seems that more studies are needed to define a protocol for optimal imaging of peri-implant buccal bone.

In conclusion, within the limits of this experimental study we can conclude that the radiographic accuracy to identify peri-implant

buccal bone with multi-slice and cone-beam CT devices is equivalent but significantly affected by the buccal bone thickness and the presence of peri-implant marginal defects. In fact, when bone thickness is ≤ 1 mm, the probability of positive identification is low with a clear tendency to its underestimation.

Acknowledgements: We would like to thank Miguel Fernández-Enríquez for his technical support on the radiographic analysis of the samples. Also, we are grateful to Institut Straumann AG for supplying the dental implants for this study.

References

- Benic, G.I., Mokti, M., Chen, C.J., Weber, H.P., Hämmerle, C.H. & Gallucci, G.O. (2012) Dimensions of buccal bone and mucosa at immediately placed implants after 7 years: a clinical and cone beam computed tomography study. *Clinical Oral Implants Research* **23**: 560–566.
- Benic, G.I., Sancho-Puchades, M., Jung, R.E., Deyhle, H. & Hämmerle, C.H. (2013) In vitro assessment of artifacts induced by titanium dental implants in cone beam computed tomography. *Clinical Oral Implants Research* **24**: 378–383.
- Buser, D., Chappuis, V., Bornstein, M.M., Wittneben, J.G., Frei, M. & Belser, U.C. (2013a) Long-term stability of contour augmentation with early implant placement following single tooth extraction in the esthetic zone: a prospective, cross-sectional study in 41 patients with a 5- to 9-year follow-up. *Journal of Periodontology* **84**: 1517–1527.
- Buser, D., Chappuis, V., Kuchler, U., Bornstein, M.M., Wittneben, J.G., Buser, R., Cavusoglu, Y. & Belser, U.C. (2013b) Long-term stability of early implant placement with contour augmentation. *Journal of Dental Research* **92**: 176S–182S.
- Chiodo, T.A., Ziccardi, V.B., Janal, M. & Sabitini, C. (2006) Failure strength of 2.0 locking versus 2.0 conventional Synthes mandibular plates: a laboratory model. *The International Journal of Oral and Maxillofacial Surgery* **64**: 1475–1479.
- Choi, B.H., Huh, J.Y., Suh, C.H. & Kim, K.N. (2005) An in vitro evaluation of miniplate fixation techniques for fractures of the atrophic edentulous mandible. *The International Journal of Oral and Maxillofacial Surgery* **34**: 174–177.
- Degidi, M., Nardi, D., Daprile, G. & Piattelli, A. (2012) Buccal bone plate in the immediately placed and restored maxillary single implant: a 7-year retrospective study using computed tomography. *Implant Dentistry* **21**: 62–66.
- Esmaili, F., Johari, M., Haddadi, P. & Vatankhah, M. (2012) Beam hardening artifacts: comparison between two Cone Beam Computed Tomography scanners. *Journal of Dental Research, Dental Clinics, Dental Prospects* **6**: 49–53.
- Holberg, C., Steinhäuser, S., Geis, P. & Rudzki-Janson, I. (2005) Cone-beam computed tomography in orthodontics: benefits and limitations. *Journal of Orofacial Orthopedics* **66**: 434–444.
- Huynh-Ba, G., Pjetursson, B.E., Sanz, M., Cecchinato, D., Ferrus, J., Lindhe, J. & Lang, N.P. (2010) Analysis of the socket bone wall dimensions in the upper maxilla in relation to immediate implant placement. *Clinical Oral Implants Research* **21**: 37–42.
- Januário, A.L., Duarte, W.R., Barriviera, M., Mesti, J.C., Araújo, M.G. & Lindhe, J. (2011) Dimension of the facial bone wall in the anterior maxilla: a cone-beam computed tomography study. *Clinical Oral Implants Research* **22**: 1168–1171.
- Jung, R.E., Benic, G.I., Scherrer, D. & Hämmerle, C.H. (2015) Cone beam computed tomography evaluation of regenerated buccal bone 5 years after simultaneous implant placement and guided bone regeneration procedures - a randomized, controlled clinical trial. *Clinical Oral Implants Research* **26**: 28–34.
- Kehl, M., Swierkot, K. & Mengel, R. (2011) Three-dimensional measurement of bone loss at implants in patients with periodontal disease. *Journal of Periodontology* **82**: 689–699.
- Lee, E.A., Gonzalez-Martín, O. & Fiorellini, J. (2014) Lingualized flapless implant placement into fresh extraction sockets preserves buccal alveolar bone: a cone beam computed tomography study. *International Journal of Periodontics & Restorative Dentistry* **34**: 61–68.
- May, K.B., Edge, M.J., Russell, M.M., Razzoog, M.E. & Lang, B.R. (1997) The precision of fit at the implant prosthodontic interface. *Journal of Prosthetic Dentistry* **77**: 497–502.
- Merheb, J., Quirynen, M. & Teughels, W. (2014) Critical buccal bone dimensions along implants. *Periodontology 2000* **66**: 97–105.
- Miyamoto, Y. & Obama, T. (2011) Dental cone beam computed tomography analyses of postoperative labial bone thickness in maxillary anterior implants: comparing immediate and delayed implant placement. *International Journal of Periodontics & Restorative Dentistry* **31**: 215–225.
- Nisapakulorn, K., Suphanantachat, S., Silkosessak, O. & Rattanamongkolgul, S. (2010) Factors affecting soft tissue level around anterior maxillary single-tooth implants. *Clinical Oral Implants Research* **21**: 662–670.
- Razavi, T., Palmer, R.M., Davies, J., Wilson, R. & Palmer, P.J. (2010) Accuracy of measuring the cortical bone thickness adjacent to dental implants using cone beam computed tomography. *Clinical Oral Implants Research* **21**: 718–725.
- Schulze, R.K., Berndt, D. & d'Hoedt, B. (2010) On cone-beam computed tomography artifacts induced by titanium implants. *Clinical Oral Implants Research* **21**: 100–107.
- Schulze, R., Heil, U., Gross, D., Bruellmann, D.D., Dranischnikow, E., Schwanecke, U. & Schoemer, E. (2011) Artefacts in CBCT: a review. *Dento-maxillofacial Radiology* **40**: 265–273.
- Schwarz, M.S., Rothman, S.L., Rhodes, M.L. & Chafetz, N. (1987a) Computed tomography: part I. Preoperative assessment of the mandible for endosseous implant surgery. *International Journal of Oral & Maxillofacial Implants* **2**: 137–141.
- Schwarz, M.S., Rothman, S.L., Rhodes, M.L. & Chafetz, N. (1987b) Computed tomography: part II. Preoperative assessment of the maxilla for endosseous implant surgery. *International Journal of Oral & Maxillofacial Implants* **2**: 143–148.
- Schwarz, F., Sahm, N. & Becker, J. (2012) Impact of the outcome of guided bone regeneration in dehiscence-type defects on the long-term stability of peri-implant health: clinical observations at 4 years. *Clinical Oral Implants Research* **23**: 191–196.
- Shiratori, L.N., Marotti, J., Yamanouchi, J., Chilvarquer, I., Contin, I. & Tortamano-Neto, P. (2012) Measurement of buccal bone volume of dental implants by means of cone-beam computed tomography. *Clinical Oral Implants Research* **23**: 797–804.
- Shmueli, K., Thomas, D.L. & Ordidge, R.J. (2007) Design, construction and evaluation of an anthropomorphic head phantom with realistic susceptibility artifacts. *Journal of Magnetic Resonance Imaging* **26**: 202–207.
- Spin-Neto, R., Gotfredsen, E. & Wenzel, A. (2013) Impact of voxel size variation on CBCT-based diagnostic outcome in dentistry: a systematic review. *Journal of Digital Imaging* **26**: 813–820.
- Spin-Neto, R., Marcantonio, E., Jr, Gotfredsen, E. & Wenzel, A. (2011) Exploring CBCT-based DICOM files. A systematic review on the properties of images used to evaluate maxillofacial bone grafts. *Journal of Digital Imaging* **24**: 959–966.
- Spray, J.R., Black, C.G., Morris, H.F. & Ochi, S. (2000) The influence of bone thickness on facial marginal bone response: stage 1 placement through stage 2 uncovering. *Annals of Periodontology* **5**: 119–128.
- Teughels, W., Merheb, J. & Quirynen, M. (2009) Critical horizontal dimensions of interproximal and buccal bone around implants for optimal aesthetic outcomes: a systematic review. *Clinical Oral Implants Research* **20**: 134–145.
- Vera, C., De Kok, I.J., Chen, W., Reside, G., Tynsdall, D. & Cooper, L.F. (2012) Evaluation of post-implant buccal bone resorption using cone beam computed tomography: a clinical pilot study. *The International Journal of Oral & Maxillofacial Implants* **27**: 1249–1257.
- Zhang, Y., Zhang, L., Zhu, X.R., Lee, A.K., Chambers, M. & Dong, L. (2007) Reducing metal artifacts in cone-beam CT images by preprocessing projection data. *International Journal of Radiation Oncology, Biology, Physics* **67**: 924–32.